A Method of Dynamic Analysis of Iodine-123-Metaiodobenzylguanidine Scintigrams in Cardiac Mechanical Overload Hypertrophy and Failure

Mark A. Rabinovitch, Colin P. Rose, Andreas J. Schwab, David H. Fitchett, George N. Honos, James A. Stewart, Luis F. Chen, Elia P. Castilla, Alvaro A. Gomez and Michal Abrahamowicz

McGill University and the Departments of Cardiology at the Montreal General Hospital, Royal Victoria Hospital, and Sir Mortimer B. Davis Jewish General Hospital, Montreal, Quebec, Canada

Cardiac sympathetic neuronal degeneration accompanies mechanical overload heart failure. We hypothesized that sympathetic nerve and myocyte failure share a common etiology and that ^{123}I-metaiodobenzylguanidine (MIBG) might provide a precise method of detecting failure in chronic mechanical overload. Our aim was to develop a method for the dynamic analysis of ^{123}I-MIBG scintigrams which could yield a quantitative index of myocardial sympathetic neuronal function in this condition. We performed serial ^{123}I-MIBG scintigraphy in 33 volunteers, 10 orthotopic cardiac transplant recipients and 26 patients with chronic mechanical overload of the left ventricle. We constructed a compartmental model in which total heart activity represents the sum of cardiac sympathetic vesicular and cytosolic pools. Patients with antecedent mechanical overload heart failure or myocardial dysfunction had accelerated myocardial egress of tracer that we ascribed to a specific impairment in vesicular storage rather than to a more rapid turnover of an intact vesicular pool.

J Nucl Med 1993; 34:589–600

When the left ventricle is exposed to a chronic mechanical overload secondary to valve disease, it hypertrophies and eventually fails due to a reduction in contractility. The proper timing of valve replacement in order to prevent irreversible left ventricular dysfunction and reduce late mortality is controversial (*1–8*). In clinical decision-making, cardiologists currently rely on both the severity of symptoms and indices of left ventricular pump performance, all of which are only imprecise reflections of cardiac myocyte integrity. We hypothesized that some biochemical index related to the possible etiology of myocyte failure might more precisely detect myocardial failure. Cardiac sympathetic nerves demonstrate depressed synthetic and transport function in mechanical overload heart failure (*9–12*). A common factor, such as tissue hypoxia, might account for the concomitant dysfunction of myocytes and adjacent interstitial sympathetic nerve fibres. On this basis, we sought a noninvasive radionuclide method to detect cardiac sympathetic denervation in mechanical overload heart failure. A synthesized compound, metaiodobenzylguanidine (MIBG), shares many cellular transport properties with norepinephrine, including neuron-specific uptake-1 (*13*), granular storage (*14,15*) and secretion in response to acetylcholine (*16*). Unlike norepinephrine, MIBG is virtually nonmetabolizable (*17*) and therefore is stored extravesicularly within the neuronal cytoplasm (*18,19*). We showed that ^{131}I-MIBG scintigraphic findings reflect the integrity of the cardiac sympathetic neuronal transport system in a canine model of mechanical overload heart failure (*20*). Specifically, failure dogs demonstrated an accelerated early left ventricular tracer efflux rate and reduced late left ventricular tracer accumulation, whereas compensated hypertrophy dogs showed normal tracer kinetics. In the present study, our goal was to develop a method of dynamic analysis of MIBG scintigrams that could be applied to patients with chronic mechanical overload of the left ventricle.

METHODS

Subjects

In order to provide a full spectrum of cardiac sympathetic nerve function for our model development, we studied three groups of patients. The first group consisted of 33 healthy volunteers of whom 20 received clonidine pre-medication (Group 1A) and 13 did not (Group 1B). Group 1A consisted of 7 females and 13 males with a mean age of 47 ± 12 yr (range 28–61 yr) and Group 1B consisted of 4 females and 9 males with a mean age of 47 ± 12 yr (range 28–61 yr). The second group consisted of 10

Received Jul. 8, 1992; revision accepted Dec. 2, 1992.

For correspondence or reprints contact: Dr. Mark Rabinovitch, Division of Cardiology, Montreal General Hospital, 1650 Cedar Ave., Montreal, PQ H3G 1A4, Canada.

orthotopic cardiac transplant recipients. There were 10 men with a mean age of 51 ± 13 yr (range 22–66 yr). They were studied a mean of 18 ± 13 mo after transplantation (range 4–41 mo). Group 2 transplant recipients were well compensated without clinical evidence of rejection at the time of study. The third group consisted of 26 patients with chronic mechanical left ventricular overload, 20 males and 6 females with a mean age of 49 ± 13 yr (range 23–68 yr). There were 18 patients with moderately severe or severe aortic insufficiency as the principal lesion, 6 patients with moderately severe or severe mitral insufficiency as the dominant lesion, one patient with combined moderate aortic insufficiency and moderate aortic stenosis and one patient with critical aortic stenosis. Two patients with aortic insufficiency were studied twice with intervening time intervals of 15 and 18 mo. All were free of concomitant hypertensive, pericardial and cardiomyopathic disease. Coronary artery disease was present in one patient with severe aortic insufficiency. However, no stenosis greater than 70% was present in this patient. Coronary artery disease was excluded by contrast angiography in 11 patients. In the remaining 14 patients, anginal symptoms and electrocardiographic criteria for coronary disease were absent.

Subject Preparation

Each subject avoided over-the-counter cold and cough remedies for 1 wk and caffeine for 1 day prior to testing. Beginning the day before testing, they ingested 100 mg of potassium iodide per day for 8 consecutive days. After an overnight fast, they lay supine and an intravenous catheter was placed in an antecubital vein. Thirty minutes later, blood was withdrawn for plasma norepinephrine determination by radioenzymatic assay (*21*). Next, oral clonidine was administered to all Group 1A, 2 and 3 subjects and radionuclide imaging was started in Group 1B subjects. The clonidine dosing schedule was 0.25 mg for weight less than 50 kg, 0.3 mg for weight 50–90 kg and 0.35 mg for weight greater than 90 kg (*22*). Three hours later, all clonidine pretreated subjects had re-determination of plasma norepinephrine followed by scintigraphy. All subjects avoided caffeine, ate lightly and refrained from exercise during the imaging period.

Radionuclide Imaging

The ^{123}I-MIBG obtained from Nordion International Inc., had a specific activity of at least 10 mCi/mg, averaging 15–20 mCi/mg. There was no detectable ^{124}I contamination at the time of calibration. A rotating, large field of view gamma camera equipped with a medium-energy, parallel-hole collimator was employed (Apex 410 ECT, Elscint (Canada) Limited, Markham, Ontario, Canada). A 20% window around the 159 keV photopeak of ^{123}I was utilized.

After norepinephrine blood sampling, 8–10 mCi of ^{123}I-MIBG was injected and flushed with normal saline. Exact injected dose and residual syringe activity were recorded. The first acquisition began 15 min after tracer injection. Thirty projections were obtained for 50 sec each in a 180° circular arc extending from the 45° right anterior oblique to the 45° left posterior oblique position. All projections were acquired in word mode (in order to avoid liver data overflow) on magnetic disk using a 64 × 64 matrix (0.688 cm/pixel). Identical acquisitions were obtained at 2, 4 and 6 hr post-tracer injection. In all the Group 1A and 1B volunteers and two of the Group 3 patients, additional acquisitions were obtained at 8, 10 and 24 hr post-tracer injection. At 2, 5 and 10 min post-tracer injection and at the mid-point of each acquisition, 1 cc of blood was withdrawn for ^{123}I assay by well counter in 5 of Group 1A volunteers, all 10 Group 2 transplant recipients and 27 Group 3 patient studies. After decay-correcting and normalizing for the dose administered and weight of subject, ^{123}I blood concentrations in %kg-dose/g of blood were obtained (*23*). After each acquisition, word to byte mode conversion of the imaging data was performed with storage of the word to byte normalization factors for later computations. Next, data from each of the acquisitions were corrected for nonuniformity with a 100 million count flood, center of rotation and decay during the time of acquisition. Filtered backprojection was then performed using a ramp-Hanning filter with a cutoff value of 0.2 cycles/pixel to reconstruct 1-pixel thick transverse axial tomograms encompassing the heart, lungs and liver. Oblique angle reconstruction was then applied to the transaxial cardiac tomographic data for generation of 1-pixel thick oblique cardiac tomograms. Finally, 2-pixel thick coronal tomograms of the lungs and liver were generated from the transaxial tomographic data. All display scale factors used during image reconstruction to avoid data overflow were stored for later calculations. No attenuation or scatter correction was used.

Liver Quantification

Two-pixel thick coronal tomograms from the anterior to posterior surface of the liver were linearly interpolated down to four representative slices. The two inner slices were employed for quantification. An 8 × 2 rectangular region of interest (ROI), equidistant from the top and bottom of the liver, was automatically generated 3 pixels in from the right edge of the liver over the hot rim of hepatic activity in both slices, avoiding attenuated activity deeper within the organ. The average hepatic counts within these two ROIs were divided by two to permit direct comparison with myocardial results and were corrected for physical decay of tracer.

Lung Quantification

Two-pixel thick coronal tomograms from the apical to basal extent of the lungs were linearly interpolated down to four representative slices: anterior, antero-mid, postero-mid and posterior. The antero-mid slice encompassing the myocardium was employed for quantification. Four by five rectangular ROIs were positioned over the middle of the right lung and over the left lung just above and lateral to the left ventricular myocardium. The positions of these regions relative to the center of the left ventricular cavity were not varied over serial acquisitions. Average counts per voxel for each lung and the average for both lungs were calculated. These average pulmonary counts per voxel were divided by two to permit direct comparison with myocardial results and were corrected for physical decay of tracer.

Myocardial Quantification

One-pixel thick oblique tomograms from the subendocardial surface of the apex to 3 pixels from the outer edge of the base were linearly interpolated down to three representative slices: apical, mid and basal. The mid-ventricular slice was employed for quantification. A circular ROI was positioned around this slice. Boundaries for a septal sub-region were set by the operator on the initial +30-min acquisition and maintained for the remaining acquisitions. To minimize the effects of scattered lung and liver activities, an asymmetrical septal sub-region was cho-

sen. Its superior border was positioned at the mediastinal limit of left lung activity and its inferior border could be moved upward to make it free of any liver contamination. Then, 6° radii were automatically generated within the septal sub-region. The average counts of the three hottest consecutive voxels along each radius was determined. Then, the average counts per voxel for all septal radii were calculated and corrected for physical decay.

To assess the reproducibility of the image analysis procedure, 13 Group 1 volunteers and 10 Group 3 patients were analyzed twice.

Dynamic Analysis of MIBG Data

It has been traditional to quantitate organ washout of MIBG (*24*) and other tracers with a simple rate constant based on the semilogarithmic slope of the time-activity curve. This approach is suitable when the organ can be assumed to act as a single compartment and is not composed of more than one compartment each of which could vary in size and rate of washout. Also, the single compartment assumption gives little insight into possible alternative explanations for changes in washout rate.

We have therefore constructed a compartmental model (Fig. 1) of cytosolic and vesicular MIBG kinetics based on the following assumptions:

1. MIBG is not metabolized in significant quantities up to 25 hr in the body (*17*).
2. The sympathetic system is in a relative steady state during the time of observation.
3. Input into the cytoplasmic pool is an impulse function.
4. Sympathetic nerves to the heart cannot be selectively activated independently of the rest of the peripheral sympathetic system by reflexes involved in the response to heart failure.
5. Total heart activity represents the sum of sympathetic cytosolic and sympathetic vesicular pools.
6. Lung washout kinetics are analogous to sympathetic axonal membrane kinetics.

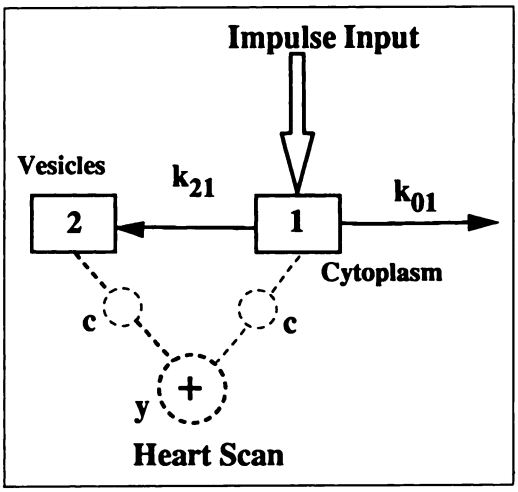

FIGURE 1. Schematic of the compartmental model used to model the heart and lung MIBG data. Total heart activity is the sum of cytosolic and vesicular compartments which have an identical attenuation. Because lung endothelium has no vesicles, it is assumed to be a pure single cytosolic compartment ($k_{21} = 0$).

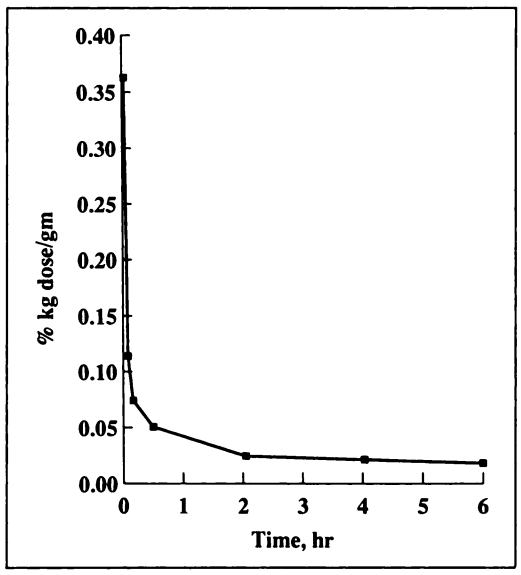

FIGURE 2. Typical ^{123}I-MIBG blood time-activity curve demonstrates the very rapid initial decrease in activity.

These assumptions require some explanation. Figure 2 shows a typical blood-time activity curve. There is a very rapid decrease in activity over the first half hour and then an almost flat, low concentration late component. We feel that this curve shape justifies to a first approximation the assumption of an impulse input into the cytoplasmic compartment of lung and sympathetic nerve cytoplasm. The rapid early decrease in activity is probably due to both rapid accumulation in the liver and in the vesicles of the peripheral sympathetic nerves.

We have demonstrated the phenomenon of localized impaired retention of MIBG by the heart independently of the spleen, a sympathetically densely innervated organ, in dogs with chronic mechanical overload heart failure (*20*). In patients with idiopathic cardiomyopathy, Glowniak et al. demonstrated very rapid cardiac washout of ^{123}I-MIBG but normal retention in the spleen and salivary glands (*24*) and interpreted the data as showing increased cardiac nerve stimulation in heart failure. If this were true, one should not see regional differences within the heart in asymmetric hypertrophy, but Nakajima et al. showed marked depression of ^{123}I-MIBG retention in the septum of patients with hypertrophic cardiomyopathy (*25*). In addition, Liang et al. have shown conclusively that sympathetic neuronal dysfunction is specific to the failing ventricle in the early stages (*26*). Although they did not remark upon it, the same phenomenon was observed by Pool et al. and Vogel et al. in one of the first investigations of this phenomenon (*9,10*). While it is improbable that cardiac nerves could be massively and selectively stimulated in early heart failure, it is even harder to believe that cardiac nerves could be stimulated selectively to the right and not the left ventricle during heart failure. Furthermore, using labeled norepinephrine and a model of norepinephrine kinetics, we previously demonstrated reduced cardiac norepinephrine release in patients with mechanical overload in spite of normal or elevated plasma norepinephrine concentrations (*12*). Besides, it has never been demonstrated in any state of reflex sympathetic activation that sympathetic nerves can be selectively stimulated to the heart and not the rest of the peripheral sympathetic system.

As an alternative explanation, we propose that there is a localized dysfunction of cardiac sympathetic nerves associated with cardiac hypertrophy and failure either due to some direct interaction between hypertrophied and failing myocytes or to some factor common to both nerves and muscle such as tissue hypoxia. Since ^{123}I-MIBG is largely stored in sympathetic vesicles when they are present (*15*), we interpret the apparent rapid washout as a failure to store ^{123}I-MIBG in vesicles rather than a rapid release of vesicles. If this is so, then we must explain the relatively normal initial MIBG uptake in the hypertrophied and failing heart (see Results). A study by Nakajo et al. provides the answer (*27*). They studied MIBG concentration in various organs of rats before and after reserpine, which selectively inhibits vesicular MIBG uptake, and found identical initial uptake after reserpine but a faster washout. While they interpreted the difference between control and postreserpine concentrations as showing the vesicular fraction, they did not take into account that MIBG is not metabolized and will accumulate in the cytoplasm when vesicular uptake is inhibited. Later, Smets et al. demonstrated this phenomenon in isolated neuroblastoma cells (*18*). Rapid washout post-reserpine is due to reverse transport or leak of MIBG across the neuronal plasma membrane and is the most probable explanation for the rapid washout in the hypertrophied and failing heart.

In the model, the lung MIBG washout kinetics are used to approximate the rate constant for egress of myocardial MIBG from the cytoplasm across the sympathetic axonal membrane, k_{01} (see Fig. 1). Lung endothelium contains the same catecholamine transporter as neuronal plasma membrane (*28,29*). Furthermore, lung endothelium concentrates MIBG by the same sodium-dependent active transport system (*30*). However, lung endothelial cells are devoid of storage vesicles and do not store biogenic amines or MIBG to any significant degree. Figure 3 shows model calculations demonstrating how cardiac neuronal MIBG content and kinetics shift as the vesicular uptake rate constant, k_{21}, decreases from 1.1 to 0 hr^{-1}. The initial uptake remains relatively constant but, as the proportion of cytosolic MIBG increases and the proportion of vesicular uptake decreases, the rate of washout increases to approach that of the lung. Thus, what looks superficially like a faster rate of vesicular release is really a decrease in vesicular storage of the nonmetabolized tracer.

The Appendix describes the mathematical treatment of the model and the equation for estimating the rate constant for vesicular uptake of MIBG by the cardiac sympathetic neurons. This index will be zero when the heart curve parallels the lung curve and some high number when the heart curve is flat. Since the upper limit is undefined, we have chosen to report the number that most closely approximates both sides of Equation A15. Two points at different times on the heart and lung curves are needed to calculate vesicular uptake. We found that the nominal 2-hr and 6-hr points gave the best discrimination between normals and patients. In some cases, the myocardial counts increase from 2 to 6 hr and in this situation it was assumed that the washout was effectively flat over this time period. In these cases, in order to compute k_{21} by an automated computer program, we found it necessary to set the 6-hr myocardial point to 99% of the 2-hr myocardial point.

Finally, we also calculated the 30-min septal myocardial-to-lung ratio and a simplified 2–6-hr septal myocardial clearance rate in percent per hour in each individual.

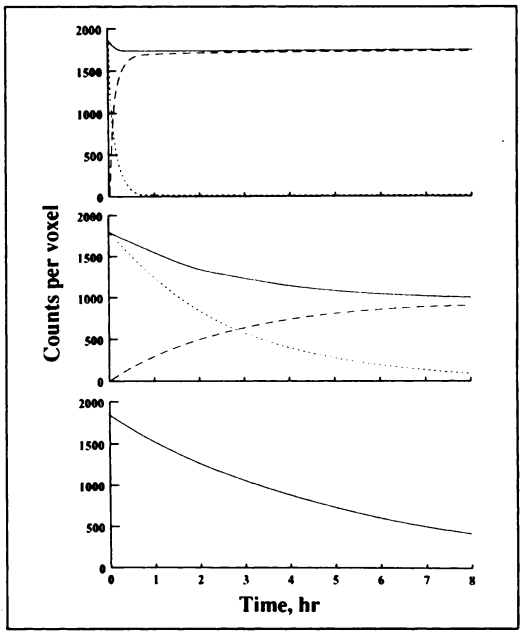

FIGURE 3. Theoretical predictions of the model for the cardiac neuronal compartment for vesicular uptake rate constants from the top down of 1.1, 0.2 and 0 hr^{-1}. The solid curve represents the sum of cytosolic and vesicular MIBG, the dotted curve the cytosolic compartment and the dashed curve the vesicular compartment. When the vesicular uptake rate is high, most of the MIBG is in the vesicles and when low it is in the cytosol and the rate of washout is increased.

Ancillary Testing

The histories of Group 3 patients were reviewed for the presence of antecedent clinical pulmonary edema and their prior chest x-rays were studied for the presence or absence of prior radiographic pulmonary edema. Each Group 3 patient underwent gated equilibrium radionuclide ventriculography within 4 mo of ^{123}I-MIBG scintigraphy.

Statistical Analysis

We performed comparisons between the groups with the unpaired t-test. A key exception was that in testing the significance of the difference in vesicular uptake between Groups 1A and 1B, we adopted a nonparametric approach due to large departures from normality, reflected in bimodal and substantially skewed distributions of vesicular uptake in both samples. We employed three nonparametric tests available in the SAS Univariate procedure (Wilcoxon rank sums, median and Kruskal-Wallis). The estimation of the normal range of vesicular uptake was based on clonidine pretreated volunteers. As the probability distribution of vesicular uptake in this sample was remarkably different from the normal ($p = 0.0001$), a standard approach, based on the assumption that approximately 95% of the values lie within two standard deviations of the mean, was inapplicable. In this situation, more flexible, nonparametric methods for probability density estimation were deemed necessary in order to account for such features as bimodality and skewness (*31*). A flexible, assumption free method based on regression splines was used since it allows for estimation of the confidence intervals in addition to point estimates of the density (*32*).

The bimodal regression spline estimate of the vesicular up-

take probability density suggested the presence of two subpopulations among normal volunteers and indicated that the cut-off point for separating these hypothetical subpopulations is close to 0.5. Given this finding, we tested for possible associations between a vesicular uptake of <0.5 and age, sex, height, weight, heart rate, blood pressure and plasma norepinephrine in all normal volunteers (n = 33) using multiple logistic regression (*33*).

To determine whether there were any systematic differences in the initial 30-min myocardial-to-lung ratio between two subgroups of valve patients with and without myocardial dysfunction and our Group 1A clonidine-pretreated volunteers, we performed one-way analysis of variance.

In our 23 reproducibility patients, we tested for systematic bias between the two sets of observations for the vesicular uptake and the 30-min myocardial-to-lung ratio using the t-test and nonparametric tests for the equality of test and retest means. We also examined test-retest reliability based on Pearson correlation analysis.

RESULTS

The results of image quantification were highly reproducible. The reproducibility study revealed no systematic bias between the two sets of observations on 23 individuals as reflected by the relative difference between test and retest means of 3.7% for vesicular uptake and 2.6% for 30-min myocardial-to-lung ratio. The high correlation coefficients of 0.98 and 0.91 for vesicular uptake and 30-min myocardial-to-lung ratios indicated excellent test-retest reliability of these measures.

The clonidine pretreatment was well tolerated in all Group 1A volunteers and Group 2 and 3 patients. Pre-tracer injection plasma norepinephrine was significantly lower in Group 1A than Group 1B volunteers (94 ± 57 versus 237 ± 92, $p < 0.001$). In combined Group 2 and 3 patients, the heart rate-systolic blood pressure product dropped by an average of 29% after clonidine (9822 ± 1827 versus 7278 ± 2081 mmHg-min^{-1}, $p < 0.0001$). Pre-tracer injection plasma norepinephrine was 117 ± 62 in Group 2 transplant patients and 114 ± 69 in Group 3 valve patients.

Clonidine pretreatment resulted in a significantly higher ^{123}I-MIBG vesicular uptake rate constant in normal volunteers. In Group 1A, the mean vesicular uptake was 0.83 hr^{-1} (range 0.12–1.11) and in Group 1B, 0.38 hr^{-1} (range 0.02–1.15, p values for nonparametric tests between 0.0025 and 0.02). However, the distribution of vesicular uptake was bimodal and negatively skewed. Fourteen Group 1A volunteers were clustered between 0.90 hr^{-1} and 1.11, while six had less than 0.50 hr^{-1}. Using the method of Abrahamowicz et al. (*32*) to establish the lower boundary of the normal range of vesicular uptake, we estimated fifth percentile of the distribution of the normal clonidine-pretreated population's vesicular uptake values to be 0.14. However, due to a relatively small sample size, the 95% confidence interval for this estimate indicated that the fifth percentile may be as low as 0.08. Therefore, we decided to declare values between 0.08 and 0.14 as equivocal and only values below 0.08 as definitely reduced.

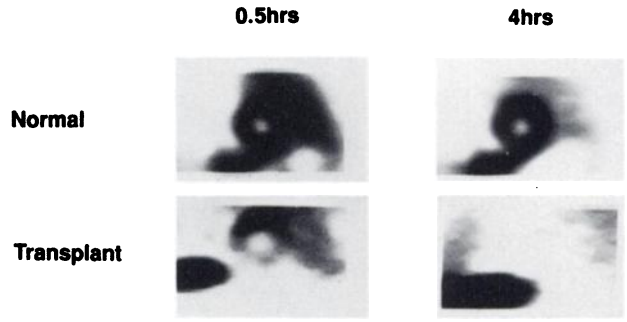

FIGURE 4. Thirty-minute and 4-hr ^{123}I-MIBG mid-ventricular scintigrams obtained in a normal volunteer (top) and a cardiac transplant patient (bottom). Note the excellent accumulation and retention of tracer in the normal volunteer and the reduced accumulation and retention in the transplant recipient.

The data also suggested the presence of two subpopulations among all normal volunteers (n = 33), with a vesicular uptake of 0.5 as the cut-off point for separating these hypothetical subpopulations. We found that, when adjusted for the effect of clonidine, only baseline resting heart rate was a significant predictor of a value <0.5, with an increase in heart rate increasing the likelihood of a low vesicular uptake (p value 0.007, whereas p values for all other factors were nonsignificant). On the other hand, even when adjusted for heart rate, clonidine pretreatment remained a significant predictor of vesicular uptake <0.5 (p value 0.015). It should also be noted that analysis of the subsample of volunteers pretreated with clonidine (Group 1A) revealed a marginally nonsignificant (p value = 0.10) association between heart rate 3 hr after drug administration and vesicular uptake < 0.5. Finally, there was no significant difference in the 30-min myocardial-to-lung ratio ($p = 0.28$) between clonidine-pretreated volunteers (1.40 ± 0.29) and nonclonidine volunteers (1.59 ± 0.58).

The distribution of the simplified 2- to 6-hr myocardial clearance rate in normal volunteers was similarly skewed. We utilized the same methodology to establish an upper limit of normal myocardial clearance of 5.36% per hour in clonidine pretreatment volunteers. Interestingly, 2- to 6-hr lung clearance had a perfectly normal distribution in volunteers and was unaffected by the drug (clonidine 9.40 ± 1.03 versus nonclonidine 8.54 ± 1.61, $p = 0.13$).

Figure 4 shows the 0.5-hr and 4-hr ^{123}I-MIBG myocardial scintigrams of a representative Group 1A volunteer and a Group 2 transplant patient. Figure 5 illustrates the corresponding liver, lung and septal myocardial time-activity curves of these individuals. In the normal case at the top, there is excellent initial accumulation and retention of tracer in the myocardium. Note the correspondingly flat myocardial time-activity curve of this individ-

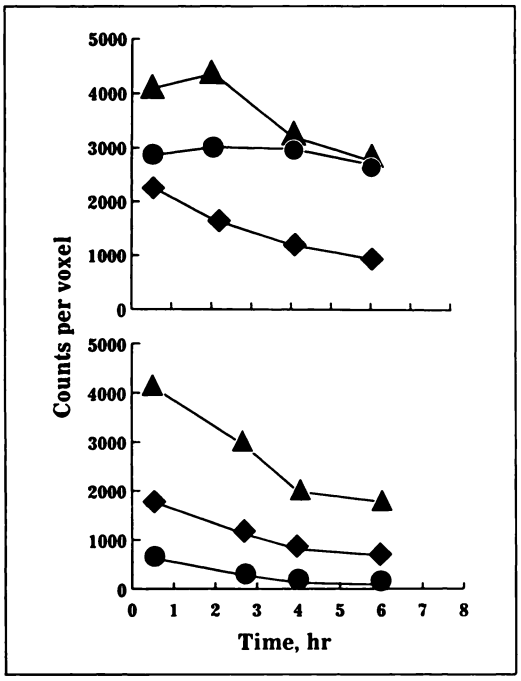

FIGURE 5. Normal and cardiac transplant time-activity curves. Iodine-123-MIBG liver (triangles), lung (diamonds) and septal myocardium (circles) time-activity curves in a normal volunteer (top) and a transplant patient (bottom). There is markedly reduced initial myocardial accumulation in the transplant recipient and rapid myocardial egress.

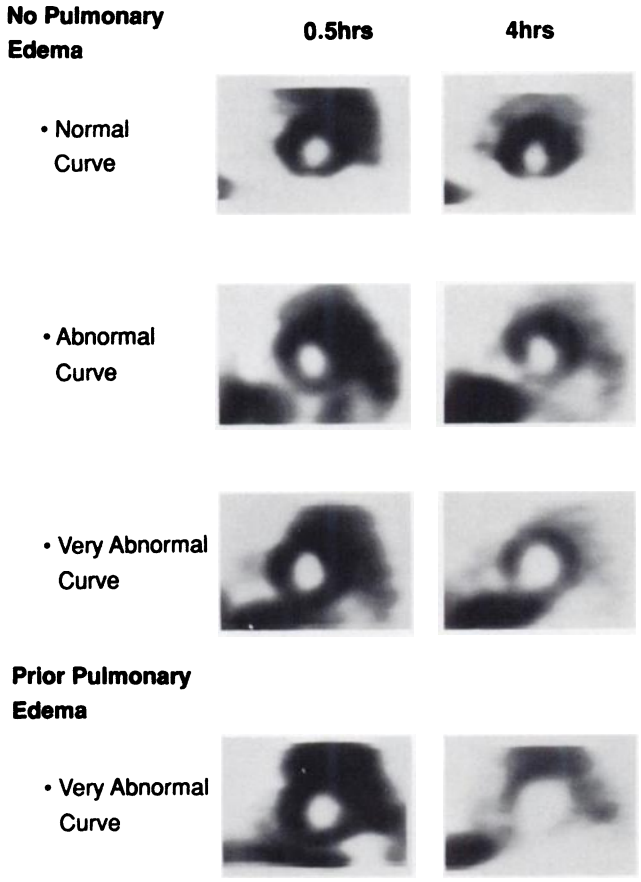

FIGURE 6. Valve patient scintigrams. Thirty-minute and 4-hr ^{123}I-MIBG mid-ventricular scintigrams obtained from three patients with regurgitant valve disease with normal systolic left ventricular performance and no antecedent pulmonary congestion (top three) and one patient with mildly reduced left ventricular ejection fraction and prior pulmonary congestion. Note the poor retention of tracer in the bottom two examples.

ual. In the transplant case at the bottom, there is markedly reduced initial accumulation and rapid disappearance over 4 hr.

There was readily visible 30-min myocardial accumulation in 6 of 10 Group 2 cardiac transplant recipients. At 30 min, there was a mean reduction of septal myocardial accumulation of 79% and at 2 hr of 91% compared to Group 1A volunteers. However, the reduction in myocardial ^{123}I-MIBG accumulation was variable. In three patients, the septal myocardial-to-lung ratio was essentially nil, whereas it exceeded 25% of normal in four other patients at 30 min after tracer injection. There was no association between the 30-min ^{123}I-MIBG septal myocardial-to-lung ratio and the number of months between scintigraphy and cardiac transplantation. Egress of ^{123}I-MIBG from the hearts of those transplant patients with quantifiable uptake were uniformly very rapid (Fig. 4).

Figure 6 depicts the 0.5-hr and 4-hr ^{123}I-MIBG myocardial scintigrams of four patients with valvular disease. The top three patients had normal left ventricular systolic pump function and effort tolerance without prior pulmonary congestion. The bottom patient had a mildly reduced left ventricular ejection fraction of 0.44 and one prior episode of pulmonary congestion. Figure 4 illustrates the corresponding liver, lung and septal myocardial time-activity curves of these individuals. All four patients show good initial accumulation of tracer. However, the top patient (no. 11) demonstrates excellent myocardial retention with no appreciable washout over 6 hr, the second patient (no. 13) shows mildly reduced retention, the third patient (no. 14) has poor retention and the fourth patient (no. 1) also has very poor retention. Note that for the latter two patients the myocardial time-activity curves parallel that of the lungs.

Table 1 summarizes the clinical and noninvasively derived indices of the Group 3 patients with chronic mechamical overload. Ten patients with either antecedent pulmonary edema or reduced resting left ventricular ejection fractions less than 0.55 in mitral insufficiency or less than 0.50 in aortic insufficiency formed a myocardial dysfunction subgroup. Their initial 30-min myocardial-to-lung ratio was 1.17 ± 0.34, whereas it was 1.22 ± 0.28 in the remaining 18 patients with normal resting left ventricular ejection fraction and no antecedent heart failure ($p = 0.64$). The differences in initial myocardial-to-lung ratios between the two patient subgroups with valvular disease and the clonidine-pretreated volunteer group, whose

TABLE 1
Clinical and Noninvasive Indices of Group 3 Patients with Chronic Mechanical Overload

	Age	Sex	MVP	CHF	NE Pre (pg/ml)	NE Post (pg/ml)	EF (%)	M/L 0.5	V.U. (hr^{-1})	Myoc clear (%/hr)
1	56	M	AI	Y	321	172	44	0.89	0.01*	10.7‡
2	55	M	AI	Y	330	88	61	1.14	0.00*	7.9‡
3	28	M	AI	N	238	123	64	1.01	0.11†	5.9‡
4	45	M	AI	N	186	94	59	1.18	0.04*	6.4‡
4r	47	M	AI	N	263	75	49	1.28	0.06*	8.5‡
5	59	M	MR	N	171	149	55	1.04	0.22	3.7
6	23	F	AI	N	281	192	60	1.87	0.09†	5.1
7	47	M	AI	N	247	72	44	0.89	0.15	3.7
8	65	F	MR	N	287	141	67	1.52	0.23	3.8
9	62	F	AI	N	217	68	66	1.57	0.20	3.0
10	68	F	AS	Y	174	47	68	1.46	0.00*	8.7‡
11	54	M	AI	N	234	96	66	1.19	0.37	2.4
12	47	M	AI	N	205	74	48	1.20	0.11†	5.6‡
13	36	M	AI	N	227	75	72	0.97	0.15	5.1
14	27	M	AI	N	259	211	59	1.15	0.00*	11.1‡
15	61	F	AS	N	175	85	72	1.18	0.32	1.1
16	39	M	AI	N	175	70	68	1.62	1.09	−0.3
17	43	M	MR	N	216	112	71	1.42	0.5	1.3
18	53	M	AI	N	243	81	65	0.72	0.85	−0.6
19	41	M	MR	Y	405	382	38	1.01	0.00*	8.0‡
20	28	M	AI	N	395	73	51	1.34	0.87	0.4
21	63	M	AI	N	230	124	44	1.29	0.20	3.4
22	61	M	MR	N	160	116	55	1.18	0.50	1.8
23	48	M	AI	N	225	147	51	0.92	0.18	4.7
23r	50	M	AI	N	283	49	56	1.11	0.26	4.2
24	65	F	MR	N	427	174	52	1.86	0.09†	6.0‡
25	44	M	AI	N	198	60	63	1.07	0.46	1.9
26	47	M	AI	N	198	52	45	0.67	0.04*	8.1‡

*†‡Definitely reduced, equivocally reduced and definitely increased, respectively.

MVP = major valve problem; AI = aortic insufficiency; MR = mitral regurgitation; AS = aortic stenosis; CHF = congestive heart failure; NEpre = plasma norepinephrine before clonidine; NEpost = plasma norepinephrine after clonidine; V.U. = rate constant for vesicular uptake of MIBG by cardiac sympathetic neurons; M/L0.5 = septal myocardial-to-lung MIBG ratio at 30 min after tracer injection; EF = radionuclide left ventricular ejection fraction; Myoc. clear. = 2- to 6-hr septal myocardial clearance.

mean ratio was 1.40 ± 0.29, were marginally nonsignificant ($p = 0.09$). Only 1 of the 10 patients in the myocardial dysfunction subgroup had an initial myocardial-to-lung ratio below the lower 95% confidence limit for the normal volunteers (Patient 26, Table 1).

The vesicular uptake index and simplified myocardial clearance rate were equally good in detecting valve patients with myocardial dysfunction as defined above. Of the 10 patients with myocardial dysfunction, six had definitely reduced vesicular uptake (including four with antecedent pulmonary edema) and two had equivocally reduced vesicular uptake. Of the 18 patients without this definition, the ^{123}I-MIBG vesicular uptake index was normal in 14, equivocally reduced in two and definitely reduced in two patients. The simplified myocardial clearance rate was normal in 15 of 18 patients with normal resting left ventricular ejection fraction and no antecedent heart failure and was abnormally rapid in 8 of 10 patients with abnormal resting left ventricular ejection fraction or antecedent heart failure.

Patient 4 with severe rheumatic aortic insufficiency but no overt pulmonary congestion showed a reduced ^{123}I-MIBG vesicular uptake of 0.04 hr^{-1} prior to a reduction in radionuclide ejection fraction from 0.59 to 0.49 in the space of 18 mo. Repeat ^{123}I-MIBG scintigraphy after this time interval continued to show a definitely reduced vesicular uptake of 0.06 hr^{-1}. This patient subsequently underwent valve replacement primarily on the basis of decreasing systolic left ventricular function. In Patient 14 with severe aortic insufficiency complicating endocarditis on a bicuspid valve, a reduced ^{123}I-MIBG vesicular uptake index of 0 was documented in the absence of congestive heart failure or reduced resting left ventricular ejection fraction. This patient eventually underwent aortic valve replacement after suffering a bland cerebral embolus.

DISCUSSION

Our model for quantifying ^{123}I-MIBG myocardial kinetics incorporates the observations we have made in normal volunteers, transplant patients and mechanical-overload patients in varying states of compensation.

Blood activity rises rapidly and falls quickly as it exchanges with the liver, lungs, cardiac and extracardiac sympathetic nerves and an extraneuronal pool located both inside and outside the heart. Later, a slow reduction of low-level blood activity reflects kidney excretion of about 50% over 24 hr (*17*). The liver has a huge capacity for initial uptake of MIBG. While this organ is a major site for catecholamine degradation, this organ does not have dense sympathetic innervation (*34*). The inability to store MIBG is manifested by the fast rate of egress of ^{123}I-MIBG from the liver in volunteers and patients alike (no difference in the rate constant for MIBG release from the liver between the groups). The initial uptake of MIBG by the lungs is also sizable. It has been shown that lung endothelium concentrates amines and MIBG by a Na^+-dependent saturable process which has the characteristics of the system for uptake across neuronal membranes, termed uptake-1 (*30*). This may account for the slower terminal egress of MIBG from the lungs compared to the liver. However, the lung endothelial cells are devoid of storage vesicles and do not store biogenic amines or MIBG to any significant extent. Therefore, egress of MIBG from the lung is relatively rapid compared to egress from the normal heart.

The very slow egress of ^{123}I-MIBG from the myocardium of normal volunteers reflects sequestration of the majority of the intraneuronal tracer within storage vesicles with a very slow release rate from this compartment. Clonidine preadministration was used for two reasons. First, we wished to remove the level of endogenous, circulating catecholamines as a confounding variable. High catecholamine levels would be expected to compete with the tracer for the specific uptake-1 sites on the sympathetic nerve membrane (*35*), but we were able to achieve low norepinephrine levels in all Group 1A volunteers and virtually all patients. Second, we had hoped to retard the release rate of ^{123}I-MIBG from storage vesicles by virtue of clonidine's central alpha 2 agonist activity (*36*). Indeed, Sisson et al. had been able to detect acute changes in cardiac MIBG washout after clonidine in four animals (*37*). Our results indicate that clonidine does retard the egress of ^{123}I-MIBG as evidenced by a significantly higher vesicular uptake rate constant in Group 1A volunteers. Nevertheless, the distribution of vesicular uptakes in Group 1A volunteers was skewed with the large majority of volunteers having values between 0.9 and 1.1 hr^{-1} and four volunteers having values less than 0.5 hr^{-1}. The most plausible explanation is that the sympathetic nervous system was incompletely inhibited by clonidine during the entire imaging period. This is supported by the significant association between vesicular uptake and baseline resting heart rate in the volunteers. Thus, while the group heart rate-blood pressure product and plasma norepinephrine were substantially reduced by clonidine at the time of tracer injection, clonidine suppression may have been incomplete in some volunteers during the course of imaging. Also, while volunteers were fasted overnight, they were permitted to eat "lightly" during the day of their study. The lack of strict food intake regulation might have resulted in sympathetic nervous activation in a minority of the volunteers (*38,39*). Lack of a striking correlation between circulating norepinephrine and MIBG kinetics may be due to measurement of plasma norepinephrine only once at the start of imaging. It could also relate to the factors involved in determining circulating norepinephrine levels and the potential differences between MIBG and norepinephrine handling. For example, Smets et al. have shown that reuptake of MIBG is more avid than that of norepinephrine and is unaffected by the frequency of cell washes in isolated neuroblastoma cells (*19*).

The data from our ten Group 2 transplant patients confirm that the heart has a very low capacity extraneuronal pool in man. Glowniak et al. showed a 94% reduction in 1-hr myocardial accumulation of ^{123}I-MIBG in four cardiac transplant patients (*24*). Dae et al. demonstrated no cardiac localization of MIBG on early imaging between 5 and 15 min after tracer injection in ten transplant patients (*40*).

One might question whether the small 30-min uptake observed in six of our transplant patients was due to sympathetic reinnervation. While some data suggest that cardiac sympathetic reinnervation is nonexistent in man (*41,42*), other recent data suggest that partial reinnervation may occur in some patients after 1 yr, primarily in the basal anterior wall (*43,44*). We quantified the midseptal wall, an area where sympathetic reinnervation has not been clearly demonstrated (*44*). Furthermore, the very rapid egress of tracer from this area suggests that we were sampling almost exclusively from a very poorly retentive extraneuronal compartment. Since the transplant myocardial accumulation of ^{123}I-MIBG was so low by 2 hr after injection (91% reduction), we decided that inclusion of the extraneuronal pool in our compartmental model was unnecessary.

The difference in the initial myocardial accumulation of tracer between our valve patients with and without myocardial dysfunction and our normal volunteers might have reached statistical significance with larger numbers of patients. However, these small group differences are unlikely to have clinical significance since 9 of our 10 valve patients with myocardial dysfunction had 30-min myocardial-to-lung ratios above the lower 95% confidence limits for normal volunteers.

Since the uptake of tracer norepinephrine is depressed in mechanical overload heart failure, reflecting an im-

paired uptake-1 process (*12,26*), one might question the lack of importantly depressed initial ^{123}I-MIBG myocardial uptake in our patients with myocardial dysfunction. It has been shown in human neuroblastoma cells that MIBG has a significantly higher affinity for uptake-1 than norepinephrine (*18*). Therefore, it may not be until the late stages of mechanical overload failure, when the uptake-1 process is severely impaired, that initial myocardial accumulation of MIBG will be clearly reduced. We did observe a patient (no. 26, Table 1) with a severely dilated and hypofunctioning left ventricle due to aortic insufficiency who had a significantly reduced initial myocardial-to-lung ratio.

We attribute the abnormally fast myocardial egress rates of ^{123}I-MIBG from our patients with myocardial dysfunction due to mechanical left ventricular overload to an impaired vesicular uptake mechanism in the failing myocardium. Vesicular storage is highly energy-dependent and might be expected to be impaired in mechanically overloaded hearts that are failing due to energy starvation. This interpretation is supported by the prior study by Nakajo et al. in which chronic reserpine administration to rats resulted in accelerated myocardial egress of MIBG paralleling lung egress but in unchanged initial accumulation (*27*). This is due to the shorter half-life of intracytoplasmic but extravesicular MIBG than intravesicular MIBG. The reason reserpine does not deplete MIBG accumulation in the myocardium as it does norepinephrine is that cytoplasmic MIBG is nonmetabolizable, whereas cytoplasmic norepinephrine is rapidly metabolized to dihydrophenylglycol by monoamine oxidase.

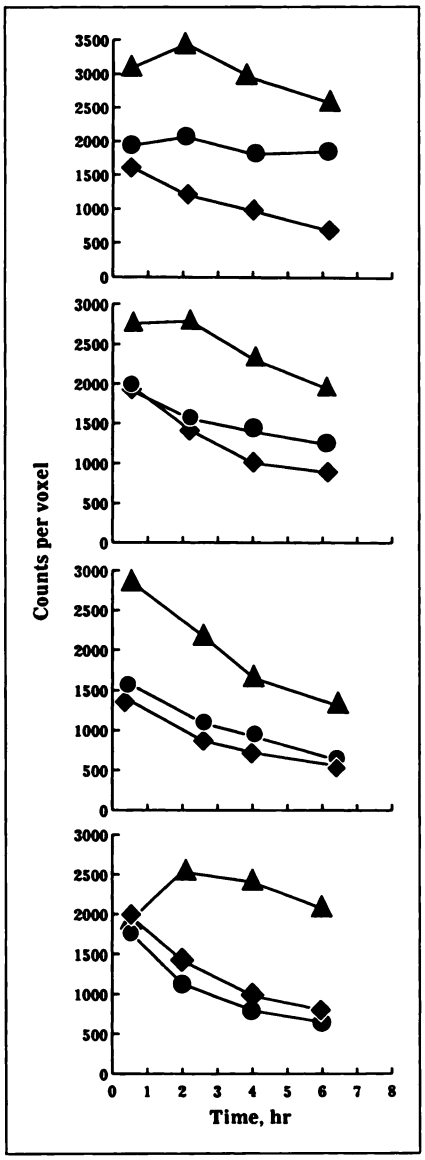

FIGURE 7. Valve patient time-activity curves. Iodine-123-MIBG liver (triangles), lung (diamonds) and septal myocardium (circles) time-activity curves of valve Patients 11 (top), 13 (second from top), 14 (second from bottom) and 1 (bottom). Patients 11, 13 and 14 have not had antecedent heart failure. Note that Patient 13 has mildly impaired and Patient 14 has severely impaired myocardial retention of tracer. Patient 1 has had prior heart failure with an LVEF = 44%. Note the severely impaired myocardial retention of tracer in this patient.

An alternative explanation for the accelerated myocardial egress of MIBG in mechanical overload heart failure is heightened sympathetic neuronal activity and a more rapid turnover of an intact vesicular pool. Our model would fit the abnormal scintigraphic data equally well with a fixed vesicular uptake and a variable vesicular release as it would with a variable vesicular uptake and a fixed vesicular release rate. However, with the former approach, up to ten-fold increases in vesicular release rates would have been required to fit the scintigraphic data. We considered these rates of release untenable for three reasons. First, pre-tracer injection catecholamine levels were relatively low due to clonidine preadministration in these patients, negating the possibility of severely heightened sympathetic nervous system activity at the time of the study. Second, markedly heightened vesicular release should have resulted in significantly increased blood ^{123}I-MIBG concentrations. To the contrary, the subgroup of patients with rapid myocardial washout of ^{123}I-MIBG did not have significantly increased blood concentrations of tracer compared to normal volunteers (Fig. 8). Third, if there were a generalized heightened sympathetic nervous activity and resultant increased MIBG turnover in the vesicular pool, the excellent retention of MIBG by other organs with dense sympathetic innervation, like the spleen and salivary glands which we and others have observed in other heart failure models, would not be seen (*20,24*).

One of our four patients with mechanical overload failure (no. 2) did have some coronary disease in addition to severe aortic regurgitation. While none of his coronary lesions were more than 70%, we cannot rule out the possibility that they played a role in the genesis of his heart failure.

The majority (14/18) of our mechanically overloaded patients without antecedent pulmonary edema or reduced left ventricular ejection fraction had normal ^{123}I-MIBG vesicular uptake. We believe that this is due to a well compensated state of myocardial hypertrophy without failure.

Two patients had fairly clear-cut abnormalities in vesicular uptake at a time when their systolic left ventricular pump function was normal. In Patient 4, the ^{123}I-

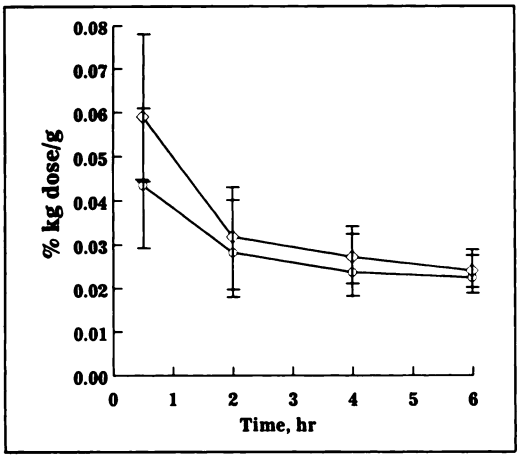

FIGURE 8. Blood concentrations in normals and patients with accelerated myocardial washout. Mean ^{123}I-MIBG blood time-activity curves of normal volunteers (diamonds) and valve patients with accelerated myocardial tracer washout (circles). Blood concentrations are expressed in %/kg-dose/g of blood. Note the lack of significantly increased blood concentrations in the subgroup of patients with accelerated myocardial washout.

MIBG scintigraphic abnormality clearly antedated a significant fall in the left ventricular ejection fraction to subnormal values over an 18-mo period. In both patients, surgical intervention precluded further follow-up to see whether clinical cardiac failure would have supervened. It is quite plausible that impairment in MIBG vesicular storage was a marker of early myocardial failure in these two patients. Clearly, the next step in the validation of ^{123}I-MIBG scintigraphy for the early detection of mechanical overload left ventricular failure is a long-term follow-up study.

It is possible that, due to incomplete suppression of sympathetic nervous activity by clonidine, the assumption of our model that there is no vesicular release during the 6 hr of imaging was violated in some patients. With even tighter control of sympathetic nervous activity during imaging in the future, improved separation of patients into clearly normal or abnormal vesicular uptake may be possible.

In general, the simplified myocardial clearance rate gave similar results to vesicular uptake in the valve patient group. While the two indices are highly interdependent, we prefer vesicular uptake at present. Lung clearance rate serves as an internal reference in computing an index of sympathetic neuronal function. Vesicular uptake better reflects the mechanism which we favor as the explanation for abnormal MIBG kinetics in mechanical overload heart failure.

Finally, we hypothesized from these results that ^{123}I-MIBG scintigraphy might prove useful for the early detection of volume overload myocardial failure and thus have a role in timing surgical intervention. It will require a prospective trial of patients with rigid entrance criteria and long-term follow-up to prove or disprove this hypothesis.

APPENDIX

Description of the Compartmental Model

We assume that the behavior of the myocardium is described by a two-compartment system, where compartment one represents the cytosol and compartment two represents vesicles (Fig. 1). We further assume bolus input into compartment one and one output consisting of the sum of both compartments, scaled with a factor c.

The behavior of this system is then described by a system of linear ordinary differential equations with constant coefficients, as follows (*45,46*):

$$\mathbf{dx/dt = Ax + Bu} \qquad \text{Eq. A1}$$

$$\mathbf{y = Cx,} \qquad \text{Eq. A2}$$

where t is time, **x** is a vector with elements x_1 and x_2 representing the contents of compartments one and two, respectively, u is the input to the system (assumed to be approximated by a delta function, y is the output representing the observations and **A**, **B** and **C** are constant matrices. According to the actual model, we set

$$u = \delta(t), \qquad \text{Eq. A3}$$

$$\mathbf{A} = \begin{pmatrix} -(k_{21} + k_{01}) & 0 \\ k_{21} & 0 \end{pmatrix} \qquad \text{Eq. A4}$$

$$\mathbf{B} = \begin{pmatrix} 1 \\ 0 \end{pmatrix} \qquad \text{Eq. A5}$$

$$\mathbf{C} = (c \quad c), \qquad \text{Eq. A6}$$

where δ is the impulse function, and c is a constant which depends on the amount injected, the proportion of tracer taken up by the myocardium and the attenuation due to the counting. The transfer function, H, of the system is then given by

$$H = \mathbf{C}(s\mathbf{I} - \mathbf{A})^{-1}\mathbf{B}, \qquad \text{Eq. A7}$$

where **I** is a unit matrix. By substituting the above definitions of **A**, **B** and **C**, one obtains:

$$H = \frac{ck_{21} + cs}{s^2 + (k_{21} + k_{01})s}. \qquad \text{Eq. A8}$$

On the other hand, if the output can be expressed as a sum of two exponentials:

$$y = a_1e^{\lambda_1 t} + a_2e^{\lambda_2 t} \qquad \text{Eq. A9}$$

the transfer function is the Laplace transform of this:

$$H = \frac{a_1}{s - \lambda_1} + \frac{a_2}{s - \lambda_2}, \qquad \text{Eq. A10}$$

which expands to:

$$H = \frac{-\lambda_1a_2 - \lambda_2a_1 + (a_2 + a_1)s}{s^2 - (\lambda_2 + \lambda_1)s + \lambda_2\lambda_1}. \qquad \text{Eq. A11}$$

Relationships between the parameters of the compartmental system, k_{21}, k_{01}, and c, and the observed coefficients of the multiexponential observations, a_1, a_2, λ_1, λ_2, are obtained by

coefficient comparison between Equations A8 and A11. Because the system is closed (no efflux of tracer into the environment), there is no constant in the denominator in Equation A8 and we obtain $\lambda_1 = 0$. The observed curve is thus a monoexponential decay to a constant activity. The other coefficients are:

$$k_{21} = \frac{\lambda_2 a_1}{a_2 + a_1} \qquad \text{Eq. A12}$$

$$k_{01} = \frac{\lambda_2 a_2}{a_2 + a_1} \qquad \text{Eq. A13}$$

$$c = a_1 + a_2. \qquad \text{Eq. A14}$$

From the algebraic form of these equations, it is evident that the three parameters k_{21}, k_{01} and c are uniquely identifiable if a_1, a_2 and λ_2 are known. Thus, the system shown in Figure 1 is structurally identifiable (*45*).

Now, if k_{01} is given by the monoexponential decay of the lung time-activity curve and z_1 and z_2 are two points on this curve, it can be shown that the ratio of two points on the heart time-activity curve, y_1 and y_2, is given by

$$\frac{y_2}{y_1} = \frac{\dfrac{e^{-\left(k_{21} + \frac{\ln\left[\frac{z_2}{z_1}\right]}{-t_2 + t_1}\right)t_2}}{-t_2 + t_1} + \dfrac{k_{21}}{\ln\left(\frac{z_2}{z_1}\right)}}{\dfrac{e^{-\left(k_{21} + \frac{\ln\left[\frac{z_2}{z_1}\right]}{-t_2 + t_1}\right)t_1}}{-t_2 + t_1} + \dfrac{k_{21}}{\ln\left(\frac{z_2}{z_1}\right)}}. \qquad \text{Eq. A15}$$

This is a transcendental equation in k_{21} but can be solved for k_{21} by numerical methods.

ACKNOWLEDGMENTS

The authors thank Dr. George Klein for processing the plasma catecholamines. Supported by the Medical Research Council of Canada and the Quebec Heart and Stroke Foundation.

REFERENCES

1. Hancock EW. Timing of valve replacement for aortic stenosis. *Circulation* 1990;82:308–309.
2. Kandath D, Nanda NC, Miller DD, Cranney GB, Lotan CS, Pohost GM. Aortic regurgitation: the role of echocardiography, radionuclide imaging and nuclear magnetic resonance imaging in its assessment. *Curr Probl Cardiol* 1990;15:39–116.
3. Crawford MH, Souchek J, Oprian CA, et al. Determinants of survival and left ventricular performance after mitral valve replacement. *Circulation* 1990;81:1173–1181.
4. Ross Jr J. Afterload mismatch in aortic and mitral valve disease: implications for surgical therapy. *J Am Coll Cardiol* 1985;5:811–826.
5. Bonow RO, Dodd JI, Maron BJ, et al. Long-term serial changes in left ventricular function and reversal of ventricular dilatation after valve replacement for chronic aortic regurgitation. *Circulation* 1988;78:1108–1120.
6. Hochreiter C, Niles N, Devereux RB, Kligfield P, Borer JS. Mitral regurgitation: relationship of noninvasive description of right and left ventricular performance to clinical and hemodynamic findings and to prognosis in medically and surgically treated patients. *Circulation* 1986;73:900–912.
7. Bonow RO, Lakatos E, Maron BJ, Epstein SE. Serial long-term assessment of the natural history of asymptomatic patients with chronic aortic regurgitation and normal left ventricular systolic function. *Circulation* 1991;84:1625–1635.
8. Starling MR, Kirsh MM, Montgomery DG, Gross MD. Mechanisms for left ventricular systolic dysfunction in aortic regurgitation—importance for predicting the functional response to aortic valve replacement. *J Am Coll Cardiol* 1991;17:887–897.
9. Vogel JHK, Jacobowitz D, Chidsey CA. Distribution of norepinephrine in the failing bovine heart. *Circ Res* 1969;24:71–84.
10. Pool PE, Covell JW, Levitt M, Gibb J, Braunwald E. Reduction of cardiac tyrosine hydroxylase activity in experimental congestive heart failure: its role in depletion of cardiac norepinephrine stores. *Circ Res* 1967;20:349–353.
11. Rose CP, Burgess JH, Cousineau D. Reduced aortocoronary sinus extraction of epinephrine in patients with left ventricular failure secondary to long-term pressure or volume overload. *Circulation* 1983;68:241–244.
12. Rose CP, Burgess JH, Cousineau D. Tracer norepinephrine kinetics in coronary circulation of patients with heart failure secondary to chronic pressure and volume overload. *J Clin Invest* 1985;76:1740–1747.
13. Jaques Jr S, Tobes MC, Sisson JC, Baker JA, Wieland DM. Comparison of the sodium dependency of uptake of MIBG and norepinephrine in cultured bovine adrenomedullary cells. *Mol Pharmacol* 1984;26:539–546.
14. Wieland DM, Brown LE, Tobes MC, et al. Imaging the primate adrenal medullae with ^{123}I- and ^{131}I-metaiodobenzylguanidine: concise communication. *J Nucl Med* 1981;22:358–364.
15. Gasnier B, Roisin MP, Scherman D, Coornaert S, Desplanches G, Henry JP. Uptake of meta-iodobenzylguanidine by bovine chromaffin granule membranes. *Mol Pharmacol* 1986;29:275–280.
16. Jaques Jr S, Tobes MC. Comparison of the secretory mechanisms or metaiodobenzylguanidine and norepinephrine from cultured bovine adrenomedullary cells [Abstract]. *J Nucl Med* 1985;26:P17.
17. Mangner TJ, Tobes MC, Wieland DW, Sisson JC, Shapiro B. Metabolism of iodine-131 metaiodobenzylguanidine in patients with metastatic pheochromocytoma. *J Nucl Med* 1986;27:36–44.
18. Smets LA, Janssen M, Metwally E, Loesberg C. Extragranular storage of the neuron blocking agent meta-iodobenzylguanidine (MIBG) in human neuroblastoma cells. *Biochem Pharmacol* 1990;39:1959–1964.
19. Smets LA, Loesberg C, Jansen M, Metwally EA, Huiskamp R. Active uptake and extravesicular storage of m-iodobenzylguanidine in human neuroblasoma SK-N-SH cells. *Cancer Res* 1989;49:2941–2944.
20. Rabinovitch MA, Rose CP, Rouleau JL, et al. Metaiodobenzylguanidine [I-131] scintigraphy detects impaired myocardial sympathetic neuronal transport function of canine mechanical overload heart failure. *Circ Res* 1987;61:797–804.
21. Peuler JD, Johnson GA. Simultaneous single isotope radioenzymatic assay of plasma norepinephrine, epinephrine and dopamine. *Life Sci* 1977;21:625–636.
22. Goldstein DS, Levinson PD, Zimlichman R, Pitterman A, Stull R, Keiser HR. Clonidine suppression testing in essential hypertension. *Ann Intern Med* 1985;102:42–48.
23. Kirshner AS, Ice RD, Beierwaltes WH. Radiation dosimetry of 19-iodocholesterol [^{131}I]: the pitfalls of using tissue concentration data [Reply]. *J Nucl Med* 1975;16:248–249.
24. Glowniak JV, Turner FE, Gray LL, Palac RT, Lagunas-Solar MC, Woodward WR. Iodine-123-metaiodobenzylguanidine imaging of the heart in idiopathic congestive cardiomyopathy and cardiac transplants. *J Nucl Med* 1989;30:1182–1191.
25. Nakajima K, Bunko H, Taki J, Shimizu M, Muramori A, Hisada K. Quantitative analysis of I-123-meta-iodobenzylguanidine (MIBG) uptake in hypertrophic cardiomyopathy. *Am Heart J* 1990;119:1329–1337.
26. Liang CS, Fan THM, Sullebarger JT, Sakamoto S. Decreased adrenergic neuronal uptake activity in experimental right heart failure—a chamber-specific contributor to beta-adrenoceptor downregulation. *J Clin Invest* 1989;84:1267–1275.
27. Nakajo M, Shimabukuro K, Yoshimura H, et al. Iodine-131-metaiodobenzylguanidine intra- and extravesicular accumulation in the rat heart. *J Nucl Med* 1986;27:84–89.
28. Nicholas TE, Strum JM, Angelo LS, Junod AF. Site and mechanism of uptake of H3-l-norepinephrine by isolated perfused rat lungs. *Circ Res* 1974;35:670–680.
29. Rorie DK. Metabolism of norepinephrine in vitro by dog pulmonary arterial endothelium. *Am J Physiol* 1982;243:H732–H737.
30. Slosman DO, Davidson D, Brill AB, Alderson PO. I-131-metaiodobenzylguanidine uptake in the isolated rat lung: a potential marker of endothelial cell function. *Eur J Nucl Med* 1988;13:543–547.

32. Abrahamowicz M, Ciampi A, Ramsey JO. Nonparametric density estimation for censored survival data: regression spline approach. *Can J Statistics* 1992;20:171-185.
33. Hosmer D, Lerneshow S. *Applied logistic regression.* New York: Wiley; 1989.
34. Anton AH, Sayre DF. The distribution of dopamine and dopa in various animals and a method for their determination in diverse biological materials. *J Pharmacol Exp Ther* 1964;145:326-336.
35. Nakajo M, Shapiro B, Glowniak J, Sisson JV, Beierwaltes WH. Inverse relationship between cardiac accumulation of meta-^{131}I-iodobenzylguandine (I-131 MIBG) and circulating catecholamines in suspected pheochromocytoma. *J Nucl Med* 1983;24:1127-1134.
36. Houston MC. Clonidine hydrochloride: review of pharmacologic and clinical aspects. *Prog Cardiovasc Dis* 1981;23:337-350.
37. Sisson JC, Bolgos G, Johnson J. Measuring acute changes in adrenergic nerve activity of the heart in the living animal. *Am Heart J* 1991;121: 1119-1123.
38. Landsberg L, Young JB. Fasting, feeding and regulation of the sympathetic nervous system. *N Engl J Med* 1978;298:1295-1300.
39. Sisson JC, Wieland DM, Sherman P, Mangner TJ, Tobes MC, Jacques Jr S. Metaiodobenzylguandine as an index of the adrenergic nervous system integrity and function. *J Nucl Med* 1987;28:1620-1624.
40. Dae MW, Demarco T, Botvinick EH, et al. Scintigraphic assessment of MIBG uptake in globally denervated human and canine hearts—implications for clinical studies. *J Nucl Med* 1992;33:1444-1450.
41. Regitz V, Bossaller C, Strasser R, Schuler S, Hetzer R, Fleck E. Myocardial catecholamine content after heart transplantation. *Circulation* 1990;82:620-623.
42. Wharton J, Polak JM, Gordon L, et al. Immunohistochemical demonstration of human cardiac innervation before and after transplantation. *Circ Res* 1990;66:900-912.
43. Wilson RF, Christensen BV, Olivari MT, Simon A, White CW, Laxson DD. Evidence for structural sympathetic reinnervation after orthotopic cardiac transplantation in humans. *Circulation* 1991;83:1210-1220.
44. Schwaiger M, Hutchins GD, Kalff V, et al. Evidence for regional catecholamine uptake and storage sites in the transplanted human heart by positron emission tomography. *J Clin Invest* 1991;87:1681-1690.
45. Cobelli C, DiStefano III JJ. Parameter and structural identifiability concepts and ambiguities: a critical review and analysis. *Am J Physiol* 1980; 239:R7-R24.
46. DiStefano III JJ, Landaw E. Multiexponential, multicompartmental and noncompartmental modeling. I. Methodological limitations and physiological interpretations. *Am J Physiol* 1984;246:R651-R664.

NOTICE TO CONTRIBUTORS

As of July 1, 1993, all manuscripts and other editorial correspondence should be sent to the *Journal*'s new Editorial Offices. Please direct materials to:

Stanley J. Goldsmith, MD, Editor-in-Chief
Offices of The Journal of Nuclear Medicine
Memorial Sloan-Kettering Cancer Center
1275 York Ave.
New York, NY 10021.

Until June 30, 1993, editorial materials will continue to be accepted at the *Journal's* Charlestown, MA offices (listed in "Information to Authors" and on page 3A). See *Newsline*, page 29N, for related article on new *JNM* Editor-in-Chief.